*Desalination and Water Treatment*
www.deswater.com

doi: 10.5004/dwt.2018.23150

132 (2018) 226–234
November

# Enhanced sunlight-driven photocatalytic performance of ZnO prepared with the assistance of urea

Xinlu Liu, Jiufu Chen, Jianzhang Li, Junbo Zhong*, Tao Wang*

*Key Laboratory of Green Catalysis of Higher Education Institutes of Sichuan, College of Chemistry and Environmental Engineering, Sichuan University of Science and Engineering, Zigong, 643000, China, email: 34674746@qq.com (X. Liu), cjf2171@163.com (J. Chen), lyl63@sina.com (J. Li), junbozhong@163.com (J. Zhong), 3wangtao3@163.com (T. Wang)*

Received 9 April 2018; Accepted 17 September 2018

**ABSTRACT**

As a prospective photo catalyst, ZnO has attracted increasing scientific attentions. However, the practical application of ZnO has been significantly hampered by the fast recombination of the photo induced electron-hole charge pairs. Herein, to further ameliorate the photocatalytic property of ZnO, ZnO with enhanced sunlight-driven photocatalytic performance was prepared by a Sol-gel method with the assistance of urea. The results show that the separation rate of photo induced electron-hole charge pairs of ZnO prepared with the assistance of urea was remarkably promoted, supported by surface photo voltage spectroscopy (SPS) characterization. The enhanced separation rate of photo induced electron-hole charge pairs results in efficient formation of $^{\bullet}O_2^-$, certified by nitroblue tetrazolium (NBT) experiments. The increased content of $^{\bullet}O_2^-$ can accelerate the decay of rhodamine B (RhB). Moreover, the presence of urea in the synthetic system increases the content of surface hydroxyl. The photocatalytic performance can be definitely benefited from all these advantageous factors. When the molar ratio of N (in urea)/Zn is 0.5%, the ZnO prepared displays the highest photocatalytic activity.

*Keywords:* ZnO; Sol-gel method; Surface properties; Charge separation rate; Urea

## 1. Introduction

As an important II-VI group wide band gap semiconductor, ZnO has triggered increasing attentions owning to its distinguished properties, such as high electron mobility, good thermal stability, nontoxicity, low cost, abundant resources and easy synthesis [1–11]. Some researchers reported that zinc oxide (ZnO) was an alternative semi-conducting material to replace the $TiO_2$ because of its higher electron mobility in the range of 115–155 $cm^2 V^{-1} s^{-1}$, wide band gap energy of 3.37 eV and similar electronic band structure [12–15]. The electron-hole pairs will be produced when the ZnO sample is illuminated by light whose energy is larger than band gap, the electrons will jump to the conduction band (CB), leaving the holes in the valence band (VB). The generated electron-hole pairs induce afterward a series of complex reactions, leading to the complete degradation of the organic pollutants adsorbed on the surface of ZnO. Although ZnO displays superiority in photo catalysis, the practical application of ZnO has been seriously hampered by the fast recombination of photo induced electron-hole charge pairs [16–23]. According to the principle of the photo catalysis, separation of charge pairs is vital for the photo catalysis. In fact, separation of charge pairs plays a dominant role in influencing the photocatalytic performance [24–30]. Therefore, it is feasible to promote the photocatalytic performance of ZnO by accelerating the separation of the photo induced charge pairs. To achieve high separation rate of charge pairs, tremendous approaches have been executed, such as doping ions into ZnO [5,14,20,31–34], construction of heterojunctions [21,35–39] and preparation of unique morphology [7,40–42].

Photocatalytic reaction happens on the surface of a photo catalyst, the surface states such as the surface hydroxyl content, surface trapping state and porosity will in turn influence the photocatalytic performance inevitably [43,44]. Therefore, the photocatalytic performance of ZnO can be promoted by ameliorating the surface states. The

*Corresponding author.

photocatalytic behavior of a semiconductor is closely associated with photo-generated electrons and holes [45]. Most of the photo-generated electrons and holes will undergo rapid recombination and only a smack portion of the carriers migrate to the surface of semiconductor for participating in the photocatalytic reactions for the bare semiconductor. The efficient separation of photo-generated electron-hole pairs is vital in improving the photocatalytic activity of the semiconductor [45,46]. In general, high content of -OH groups on the surface of ZnO is favorable for the production of •OH radicals, thereby enhancing its photocatalytic activity [47].

Urea is a cheap and readily available raw material. Herein, we reported urea assisted sol-gel method for preparation of ZnO with remarkably enhanced photocatalytic performance by ameliorating the surface states (surface hydroxyl content and surface trapping state), the presence of urea in the synthetic system alters the surface trapping state and increases the -OH group on the surface. The results demonstrate that urea assisted sol-gel preparation of ZnO is an effective and feasible method to ameliorate the photocatalytic of ZnO. Hopefully, the results of this work can provide a promising photo catalyst for the degradation of organic dyes and other hazardous substances.

## 2. Experimental section

### 2.1. Preparation of the samples

ZnO photo catalysts were prepared via a sol-gel method as described in the Ref. [48] with some modification. Typically, 2.19 g zinc acetate dihydrate and desired urea were dissolved in 100 mL ethanol at 333 K under vigorous stirring for 30 min, forming solution A (the molar ratio of N from urea/Zn was 0%, 0.1%, 0.3%, 0.5% and 1%); 2.51 g oxalic acid was dissolved in 40 mL ethanol at 333 K, forming solution B. Solution B was slowly added to the solution A. The mixture was then stirred for 2 h until a gel was formed. The dried gel was baked in a muffle furnace at 673K for 2 h to obtain ZnO powder. The sample prepared with different molar ratios of N/Zn was marked as 0% (ZnO), 0.1%, 0.3%, 0.5%, and 1.0%, respectively.

### 2.2. Characterization of the samples

The measurements of BET specific surface area were performed on a SSA-4200 automatic surface analyzer (Builder, China). The crystal phase of the samples prepared was analyzed on a DX-2600 X-ray diffractometer using Cu Kα radiation. The morphology and energy dispersive spectrometer (EDS) of the samples were observed on a VEGA 3 SBU scanning electron microscopy (SEM) using an acceleration voltage of 15 kV. UV-vis diffuse reflectance spectra (DRS) of the samples were carried out on a TU-1907 UV-vis spectrophotometer. SPS signals were collected as the procedures given in the Ref. [49]. Experiments of X-ray photo electron spectroscopy (XPS) were taken on an XSAM 800 using Mg Kα at 12 kV and 12 mA. The $\bullet O_2^-$ was detected using Nitroblue tetrazolium (NBT) method as described in the Ref. [50].

### 2.3. Photocatalytic test

The photocatalytic properties of ZnO prepared were tested by decolorization of RhB aqueous solution (50 mL, pH = 7.0) under simulated sunlight irradiation. The detailed experimental procedures are described in [51]. The dosage of photo catalyst was 1 g/L. The light resource was a 500 W Xe lamp (simulated sunlight). At given intervals, 3 mL suspension was withdrawn and centrifuged to separate the photo catalyst, the decay of RhB aqueous solution was detected on a UV-vis spectrophotometer at 550 nm using Beer-Lambert Law.

The decolorization efficiency of RhB was obtained as follows: $\eta = (A_0 - A)/A_0 \times 100\%$, where η is the decolorization efficiency of the RhB aqueous solution; $A_0$ is the initial absorbance of the RhB solution; $A$ is the absorbance of the RhB after photocatalytic reaction.

## 3. Results and discussion

### 3.1. Characterization of the samples

For heterogeneous photo catalysis, specific surface area is one of the vital factors which influence the photocatalytic performance [30,52]. Commonly, high catalytic activity can be benefited from the relatively high specific surface area, since high specific surface area can provide more active sites [53]. Therefore, it is necessary to investigate the specific surface area of the samples. The specific surface area of the samples prepared is exhibited in Table 1. As displayed in Table 1, the specific surface area of the samples has no obvious difference, which implies that adding urea into the synthetic system of ZnO cannot effectively alter the specific surface area of ZnO prepared. Combined with the results of photocatalytic evaluation, it is evident that specific surface area performs minor role in affecting the difference in photocatalytic performance in this case.

The crystal phase can affect the photocatalytic activity of the catalyst, thus it is indispensable to study the crystal structure of the sample. The X-ray diffraction (XRD) patterns of the samples are demonstrated in Fig. 1. As displayed in Fig. 1, all strong peaks of the samples can be readily indexed as the pure hexagonal phase of wurtzite-type ZnO, which agrees well with the reported data (JCPDS No. 79-0206). No other peaks were observed, indicating that relatively high purity of ZnO prepared. This result can be further confirmed by the results of EDS and XPS. Moreover, no shift of diffraction angles of ZnO samples prepared with the assistance of urea was observed, which indicates that no C

Table 1
Specific surface area of the samples

| Photocatalyst (%) | $S_{BET}$ ($m^2/g$) |
|---|---|
| 0 | 24.4 |
| 0.1 | 24.7 |
| 0.3 | 24.8 |
| 0.5 | 25.7 |
| 1.0 | 27.9 |

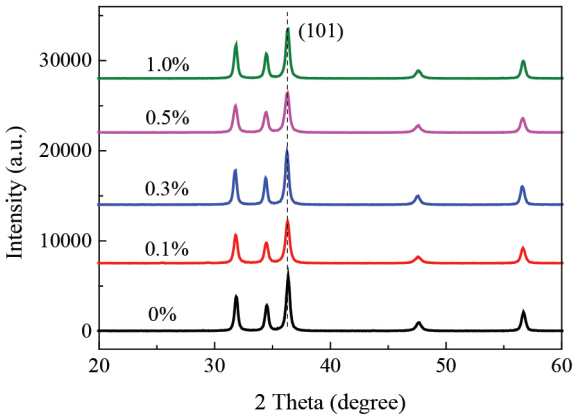


Fig. 1. XRD patterns of the samples prepared.

or N was doped into the lattice of ZnO, thus all the samples have similar crystal phase and diffraction peaks, which can be supported by the results of BET, UV-vis DRS and XPS.

To investigate the effects of the presence of urea in the synthetic system on the morphology of the samples, SEM was performed and the results are shown in Figs. 2A–D. It is interesting to find that all the samples prepared exhibit fried dough twists-like shape, suggesting that urea cannot effectively change the shape of ZnO. It is reasonable to conclude that the shape of ZnO is mainly influenced by the nature of the preparation process and precursor. During the preparation process of ZnO, urea was completely burned, thus the shape cannot be affected. Although urea cannot influence the shape of ZnO, the surface states can be facilely adjusted by the presence of urea in the synthetic system of ZnO, which can be further confirmed by the results of SPS and XPS. EDS investigation of the 1% sample is shown in Fig. 2E. As expected, only Zn and O elements were observed on the surface of the 1% sample, no N element was detected on the surface of the 1% sample, which is in good consistent with the results of XPS.

The optical property is an important parameter which influences the photocatalytic performance of the photo catalysts. Due to the overlap of the UV-vis DRS of the samples, therefore only the UV-vis DRS of the 0% and 1.0% sample are provided in Fig. 3A. As shown in Fig. 3A, considering the measurement error, the UV-vis DRS of the samples exhibit no obvious difference, which indicates that the band gap of the samples cannot effectively altered by urea, suggesting that no C or N was doped into the lattice of ZnO, thus all the samples have same band gap. The band gap of the samples can be estimated using the formula Eg=1240/λ, where λ is the adsorption edge. The adsorption edges of ZnO is 387 nm (Fig. 3B), thus the corresponding band gap of ZnO is around 3.20 eV. The CB and VB potentials of ZnO can be further calculated using the Mulliken electro negativity theory as follows:

$$E_{VB} = X - E^e + 0.5Eg$$

$$E_{CB} = E_{VB} - Eg$$

where $E_{VB}$ and $E_{CB}$ are the VB and CB band edge potential, respectively. $X$ is the absolute electro negativity of the semiconductor, which is the geometric mean of electro negativity of the constituent atoms, $E^e$ is the energy of free electrons on the hydrogen scale (~4.50 eV), and $Eg$ is the energy gap of the semiconductor. For ZnO, the $X$ value is 5.94 eV. Based on the energy gap levels, the calculated $E_{VB}$ and $E_{CB}$ of ZnO are 3.04 eV and –0.16 eV, respectively. It can be seen that the VB potential of ZnO is more positive than the $^{\bullet}OH/H_2O$ (+2.68 eV) and $^{\bullet}OH/OH^-$ (1.99 eV), so the holes generated in the ZnO VB can directly oxidize $H_2O/OH^-$ to form $^{\bullet}OH$. The standard potential of $O_2/^{\bullet}O_2^-$ is reported to be –0.046 eV, the electrons form CB of ZnO can reduce $O_2$ to generate $^{\bullet}O_2^-$. The holes and electrons can be separated effectively by formation active free radicals ($^{\bullet}O_2^-$ and $^{\bullet}OH$). Moreover, $^{\bullet}OH$, $^{\bullet}O_2^-$ and $h^+$ can attack RhB molecules, resulting in the degradation of RhB, which can be further certified by the trapping experimental results.

According to the principle of photolysis, among the steps of photocatalytic process, the separation behaviors of the photo generated electron-hole pairs play an important role in affecting the photocatalytic property [24–30]. Therefore, it is crucial to investigate the separation behaviors of the photo generated electron-hole pairs to better understand the photocatalytic property. The separation properties of the photo generated electron-hole charge pairs are demonstrated in Fig. 4, the results demonstrate that all the ZnO photo catalysts prepared with the assistance of urea hold stronger SPS signal than the reference ZnO. The dramatically enhanced SPS responses of the ZnO photo catalysts prepared with the assistance of urea reveal that the surface trapping states (surface net charge) have been promoted and the 0.1%, 0.3%, 0.5% and 1.0% samples possess more surface net charge than the reference ZnO. Commonly, surface net charge can drive the flow and separation of electrons and holes in different directions, greatly boosting the charge separation rate and resulting in stronger SPS responses [20]. Similar results were observed for preparation of $TiO_2$ and ZnO with the assistant of SDBS, $NH_4Cl$, $(NH_4)_3PO_4$ and CTAB [29,48,54,55]. Usually, rich surface trapping states can significantly enhance the photocatalytic performance of photo catalysts. Furthermore, the fact that urea alters the surface states (surface hydroxyl content) can be further certified by the results of XPS. Additionally, SPS signals of ZnO prepared with the assistance of urea gradually increase as the amount of urea increasing, and then decrease sharply. Among all these samples, the 0.5% sample exhibits the strongest SPS response. However, the reason why excessive urea will result in relative weak SPS signal needs to be further clarified. Generally, strong SPS response originates from high separation rate of the photo induced electron-hole pairs [56]. Consequently, it is apparent that the 0.1%, 0.3%, 0.5% and 1.0% samples displays higher separation rate of the photo induced electron-hole pairs than the reference ZnO, at the same time the 0.5% sample has the highest separation rate of the photo induced electron-hole pairs. Therefore, it is expected that the 0.1%, 0.3%, 0.5% and 1.0% samples will exhibit higher photocatalytic performance than the reference ZnO, which can be proved by the results of photocatalytic test.

The active free radicals during the photocatalytic decolorization of RhB were examined by adding ammonium oxalate (AO for $h^+$), isopropyl alcohol (IPA for

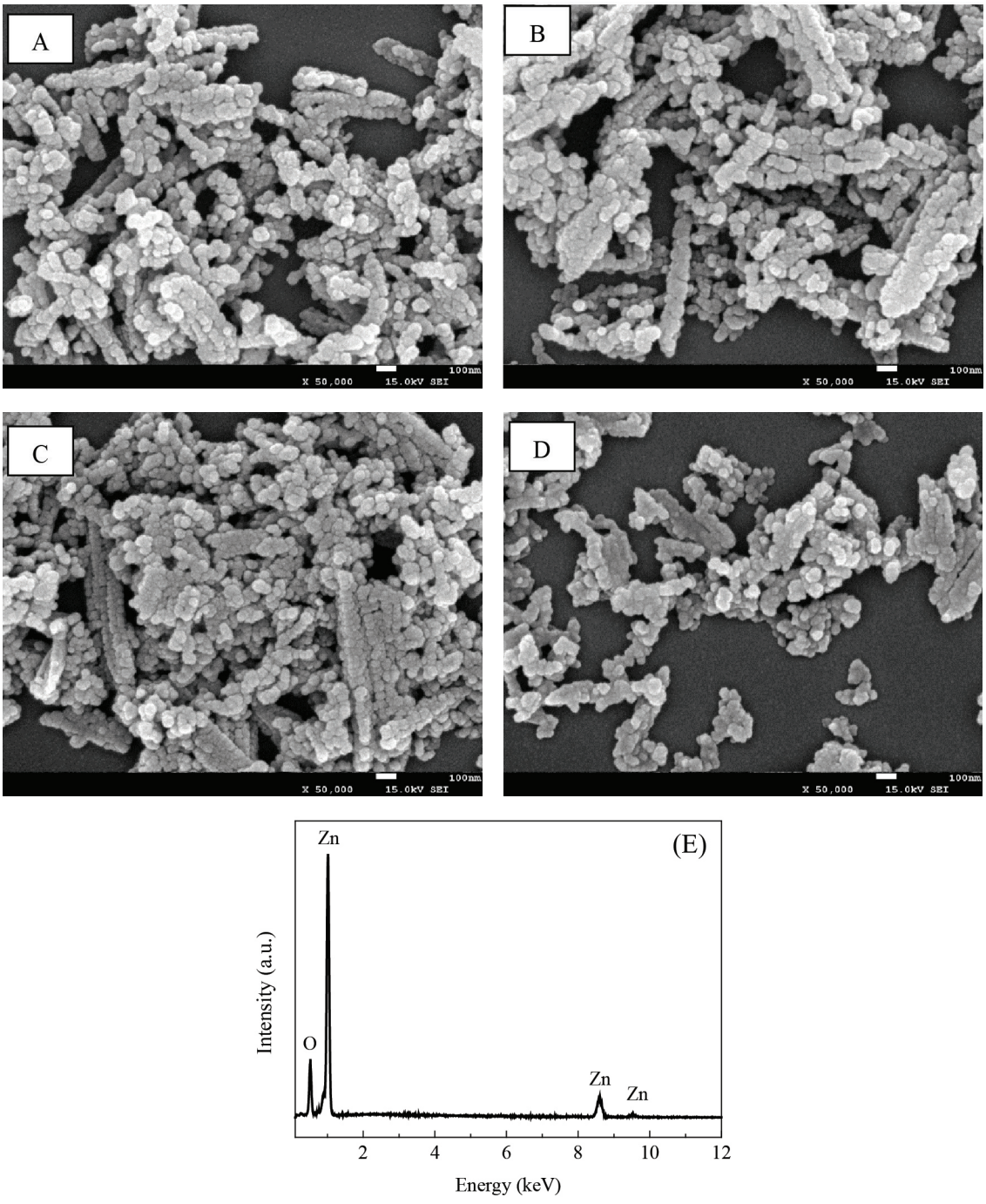


Fig. 2. SEM of the photocatalysts (A) ZnO; (B) 0.3%; (C) 0.5%; (D) 1%; (E) EDS of the 1% sample.

•OH) and benzoquinone (BQ for $^{\bullet}O_2^-$) [57] into the 0.5% photocatalytic reaction system, respectively. The results are illustrated in Fig. 5, the decolorization efficiency of RhB drops sharply due to the presence of scavengers in the photocatalytic system. As shown in Fig. 5, BQ significantly inhibits the decolorization efficiency of BhB, the decolorization efficiency of RhB over the 0.5% sample is only 20%, which firmly supports that $^{\bullet}O_2^-$ plays a leading role in photocatalytic decolorization of RhB, while •OH performs a minor role. To further investigate the effects of adding urea into the synthetic system on the formation of $^{\bullet}O_2^-$ on the surface of the different photo catalysts, NBT experiments were performed and the results are presented in Fig. 6. NBT is a water-soluble substance with absorption peak at 259 nm. Since NBT can combine with four super oxide anions to form a purple water-insoluble substance, which can conform the relative amount of $^{\bullet}O_2^-$ generated in the system [58]. As demonstrated in Fig. 6, the conversion of NBT gradually increases as the amount of urea elevating; the conversion of NBT over the 0.5% samples is the highest

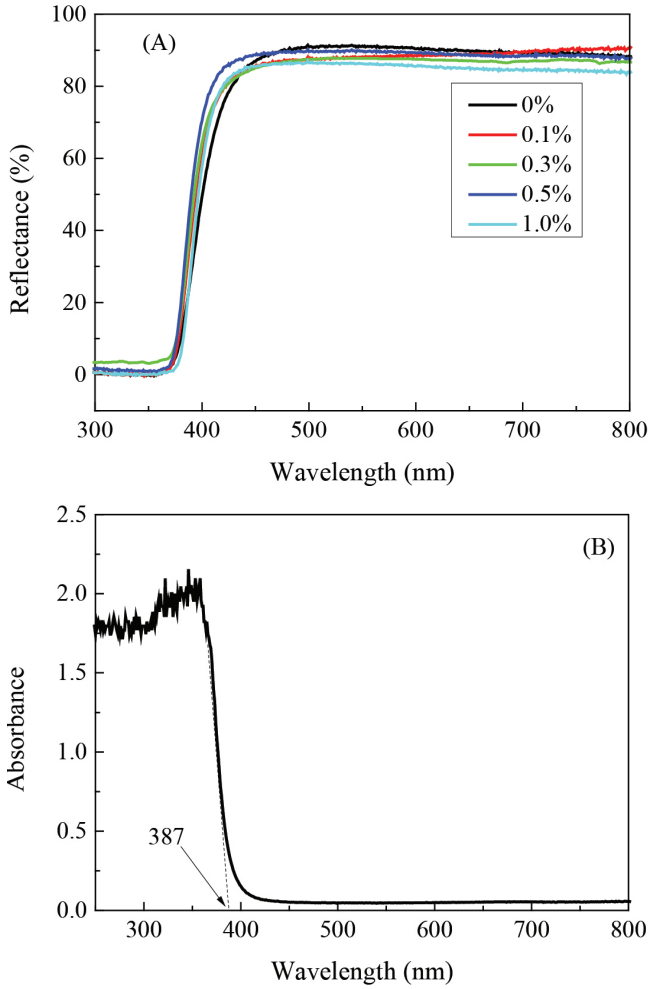


Fig. 3. (A) UV-Vis DRS of the samples prepared; (B) Adsorption edge of the 0% sample

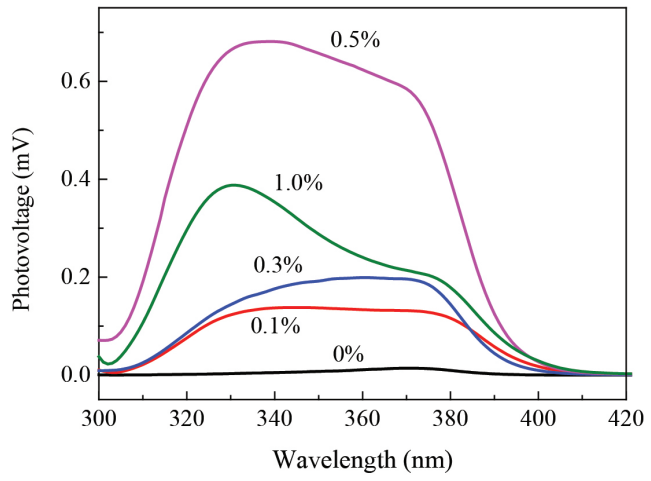


Fig. 4. SPS responses of the samples.

and then begins to drop. Due to the exclusive reaction between NBT and $^{\bullet}O_2^-$ [55], high conversion of NBT represents high content of $^{\bullet}O_2^-$ produced on the surface of photo catalyst, thus, it is evident that content of $^{\bullet}O_2^-$ on

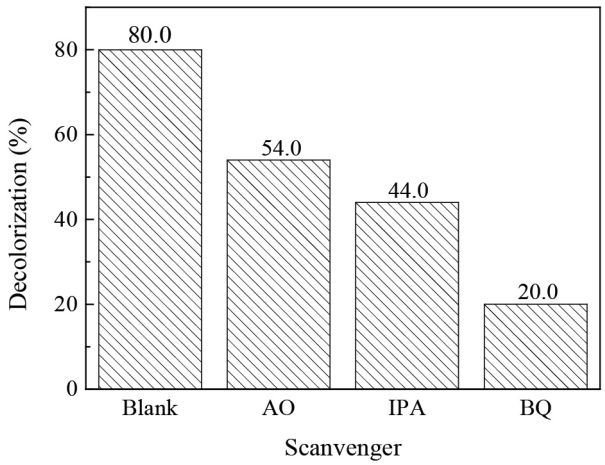


Fig. 5. Effects of scavengers on the decolorization of RhB over the 0.5% sample, the irradiation time was 20 min, the concentration of scavengers was 0.2 mmol/L.

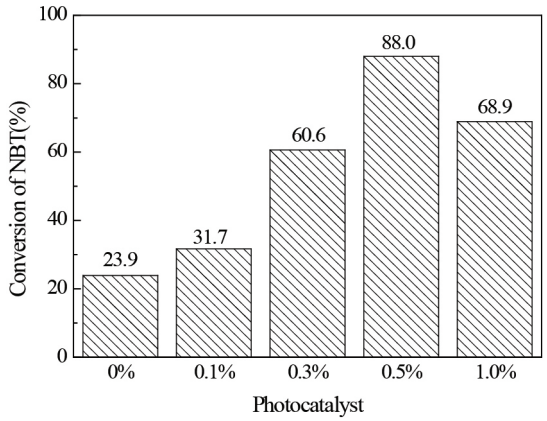


Fig. 6. Conversion of NBT over the different photo catalysts, the irradiation time was 20 min, the concentration was 0.05 mmol/L.

the 0.5% sample is the highest. However, the conversion of NBT on the 1% sample begins to drop, which can be attributed to the excessive loading of urea, the separation of photo-generated charge pairs was significantly reduced, as proven by the results of SPS. Commonly, high separation efficiency of photo-generated charge pairs and high amount of $^{\bullet}O_2^-$ are beneficial to the photocatalytic performance of photo catalyst. Since $^{\bullet}O_2^-$ takes a predominate role in decolorization of RhB, it is anticipated that the 0.5% sample will exhibit the best photocatalytic performance, according well with results of photocatalytic tests. NBT results are in good consistent of the results of SPS. $^{\bullet}O_2^-$ stems from the reaction between photo induced electrons and $O_2$ adsorbed on the surface of ZnO, high separation rate of photo generated carriers results in high content of $^{\bullet}O_2^-$.

The surface composition was further studied by XPS. Fig. 7 presents the XPS spectrum investigation of the 1% sample, as expected, C, Zn and O elements were detected. C comes from the instrument itself, Zn and O elements come from ZnO. The XPS investigation fits well with the results of EDS. Moreover, no N element was observed, indicating that N element was escaped during the baking process or the

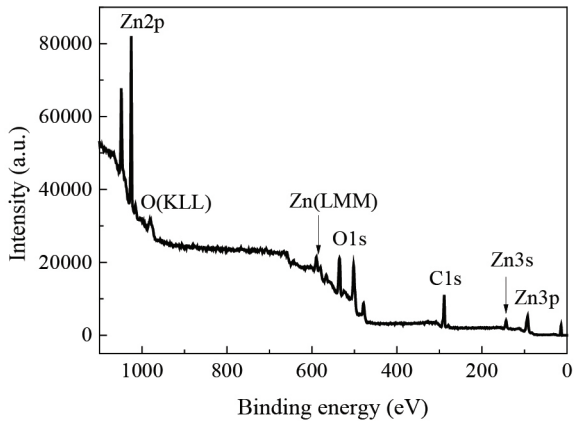


Fig. 7. XPS spectrum investigation of the 1% sample.

residual N is so small that cannot be detected by XPS, thus the effects of N on the binging energy of Zn and O can be totally ignored. The high-resolution XPS spectra of the O 1s region on the surfaces of the photo catalysts are exhibited in Fig. 8A-D. Three oxygen signals situated at 530.2 eV, 531.4 eV and 532.2 eV were observed, respectively. The O 1 s peak situated at binding energy of 530.2 eV can be assigned to the lattice oxygen of ZnO [59,60]. The peaks located at 531.4 eV can be allocated to surface-adsorbed hydroxyl groups [61–63]. The O 1 s peak at 532.2 eV is due to chemisorbed water or $O_2$ on the surface of the photo catalysts [64,65]. Table 2 presents surface hydroxyl oxygen over the four photo catalysts. It is clear the content of surface hydroxyl oxygen on 0.3%, 0.5% and 1.0% is higher than that on the 0% sample, suggesting that adding urea into the synthetic system can remarkably alter the surface properties of ZnO, boosting the surface hydroxyl groups on ZnO. However, the underlying mechanism needs to be revealed in the near future. Generally, high surface hydroxyl content on the surface of ZnO is conducive to the photocatalytic activity [31,66]. During photocatalytic process, the photo induced holes can directly attack the surface hydroxyl groups to form surface hydroxyl radicals with high oxidation ability [67]. The formed hydroxyl radicals can accelerate the decay of RhB, manifesting high photocatalytic performance.

### 3.2. Photocatalytic tests

The adsorption of RhB on different samples after 20 min in dark is exhibited in Fig. 9. As displayed in Fig. 9, the adsorption of RhB on all the photo catalysts is less than 8% and can be ignored. The photocatalytic properties of the samples are displayed in Fig. 10. It is apparent that all the ZnO samples prepared with the assistance of urea exhibit higher photocatalytic activity than the reference ZnO. Among all these photo catalysts, the 0.5% sample displays the highest photocatalytic activity. The decay of RhB over the different samples follows a first-order kinetic model. The decay rate constants of RhB over the different samples are 0.031 $min^{-1}$, 0.039 $min^{-1}$, 0.053 $min^{-1}$, 0.081 $min^{-1}$ and 0.066

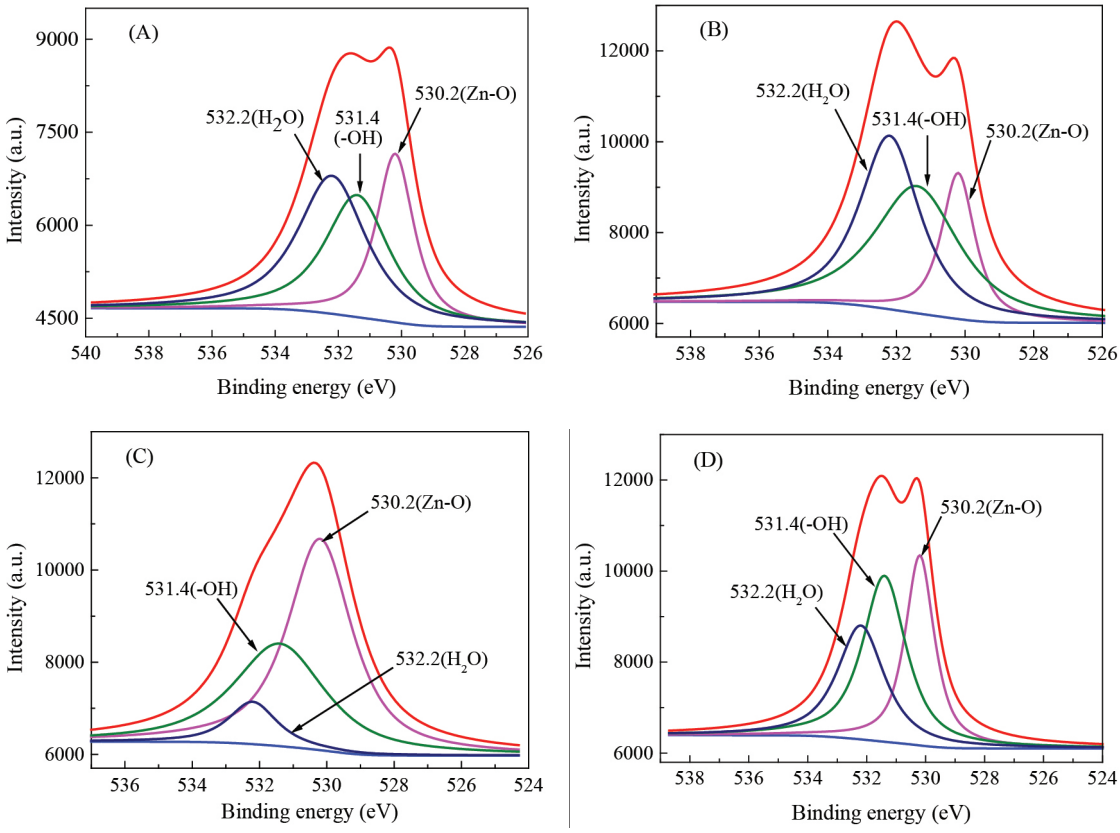


Fig. 8. O1s of the samples prepared; (A) 0%; (B) 0.3%; (C) 0.5%; (D) 1.0%.

Table 2
Surface hydroxyl oxygen over the different photo catalysts

| Sample | O1s (O-H) | |
|---|---|---|
| | $E_b$ /eV | $R_i$ /% |
| 0% | 531.4 | 33.21% |
| 0.3% | 531.4 | 41.36% |
| 0.5% | 531.4 | 37.3% |
| 1.0% | 531.4 | 39.8% |

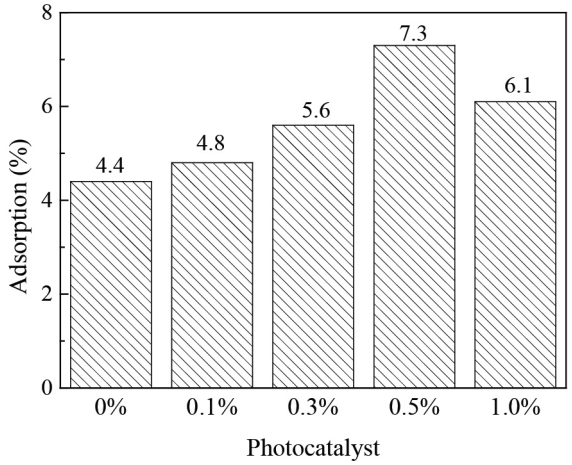


Fig. 9. Adsorption of RhB on the different photo catalysts after 20 min in dark.

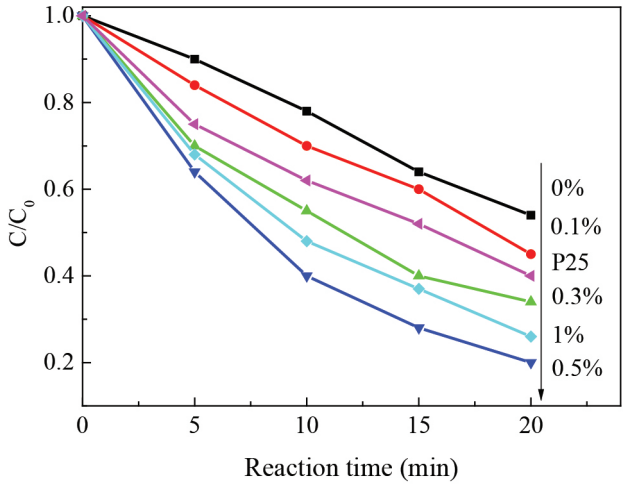


Fig. 10. Photocatalytic activities of the sample as prepared; the initial mass concentration of RhB aqueous solution was 10 mg $L^{-1}$, the initial pH value of RhB aqueous solution was 7.00, and the dosage of photo catalyst was 1 g $L^{-1}$.

$min^{-1}$, respectively. The decay rate constant of RhB over P25 is 0.044 $min^{-1}$. The photocatalytic activity performance of the 0.5% sample is more than 2.6 times of that of the 0% samples. P25 is a heterojunction composed of 80% anatase and 20% rutile $TiO_2$, which has a high photocatalytic activity. Compared to P25, the 0.5% sample exhibits higher photocatalytic activity, while the 0% and 0.1% sample display lower photocatalytic activity than P25, which can be ascribed to the different preparation approach and surface state properties. The results substantially demonstrate that preparation of ZnO with the assistance of urea is a facile and effective way to promote the photocatalytic performance of ZnO by ameliorating the surface properties.

To further investigate the photocatalytic performance of the samples prepared, the removal of COD is depicted in Fig. 11. As displayed in Fig. 11, the COD removal of RhB over the different samples gradually increases as the loading of urea increasing, and the COD removal of RhB over the 0.5% samples is the highest, and then the COD removal efficiency of RhB drops as the loading of urea further elevating. The trend is in good consistent well with the result of decay of RhB over the different photo catalysts.

Photocatalytic oxidation technology is a complex process; so many factors can affect the photocatalytic activity, such as the specific surface area, band gap, surface hydroxyl content, carriers separation rate and so on. Among all these factors, charge separation rate performs a leading role in deciding the photocatalytic performance in this case.

## 4. Conclusions

In summary, remarkably enhanced solar-driven photocatalytic performance of ZnO photo catalysts were successfully prepared by a Sol-gel method with the assistance of urea. The results display that all the ZnO photo catalysts prepared with the assistance of urea exhibit higher photocatalytic activity than the reference ZnO, benefiting from the efficient formation $^{\bullet}O_2^-$ on the ZnO surface, enhanced separation rate of the photo-induced charge pairs and increased content of surface hydroxyl. When the molar ratio of N/Zn is 0.5%, the ZnO prepared holds the highest photocatalytic activity. Preparation of ZnO with the assistance of urea is an effective way to remarkably promote the photocatalytic performance of ZnO. This method can be employed to prepare other photo catalysts with excellent photocatalytic performance.

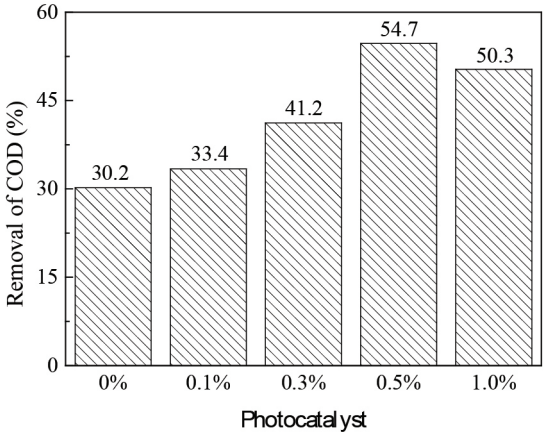


Fig. 11. COD removal of RhB over the samples under the simulated solar illumination for 20 min.

**Acknowledgments**

This project was financially supported by the Opening Project of Key Laboratory of Green Catalysis of Sichuan Institutes of High Education (No. LYJ14207).

**References**

[1] Z.X. Pei, L.Y. Ding, M.L. Lu, Z.H. Fan, S.X. Weng, J. Hu, P. Liu, Synergistic effect in polyaniline-hybrid defective ZnO with enhanced photocatalytic activity and stability, J. Phys. Chem. C., 118 (2014) 9570–9577.
[2] P.C. Patel, S. Ghosh, P.C. Srivastava, Structural, magnetic and optical properties of ZnO nanostructures converted from ZnS nanoparticles, Mater. Res. Bull., 81 (2016) 85–92.
[3] R.Y. Yang, X.X. Yan, Y.M. Li, X.H. Zhang, J.H. Chen, Nitrogen-doped porous carbon-ZnO nanopolyhedra derived from ZIF-8: New materials for photo electrochemical biosensors, ACS Appl. Mater. Interfaces, 9 (2017) 42482–42491.
[4] P.Q. Jia, H.W. Tan, K.R. Liu, W. Gao, Enhanced photocatalytic performance of ZnO/bone char composites, Mater. Lett., 205 (2017) 233–235.
[5] Y.L. Chen, L.J. Wang, W.Z. Wang, M.S. Cao, Synthesis of Se-doped ZnO nanoplates with enhanced photo electrochemical and photocatalytic properties, Mater. Chem. Phys., 199 (2017) 416–423.
[6] C. Bojer, J. Schöbel, T. Martin, M. Ertl, H. Schmalz, J. Breu, Clinical wastewater treatment: Photochemical removal of an anionicantibiotic (ciprofloxacin) by mesostructured high aspect ratio ZnO nanotubes, Appl. Catal. B: Environ., 204 (2017) 561–565.
[7] S.S.P. Selvin, A.G. Kumar, L. Sarala, R. Rajaram, A. Sathiyan, J.P. Merlin, I.S. Lydia, Photocatalytic degradation of rhodamine B using zinc oxide activated charcoal polyaniline nanocomposite and its survival assessment using aquatic animal model, ACS Sustainable Chem. Eng., 6 (2018) 258–267.
[8] H. Liu, M. Li, J. Yang, C. Hu, J. Shang, H. Zhai, In situ construction of conjugated polymer P3HT coupled hierarchical ZnO composite with Z-scheme enhanced visible-light photocatalytic activity, Mater. Res. Bull., 106 (2018) 19–27.
[9] M.Y.N. Núñez, A.M. Cruz, Nitric oxide removal by action of ZnO photo catalyst hydrothermally synthesized in presence of EDTA, Mat. Sci. Semicon. Proc., 81 (2018) 94–101.
[10] P. Pascariu, I.V. Tudose, M. Suchea, E. Koudoumas, N. Fifere, A. Airinei, Preparation and characterization of Ni, Co doped ZnO nanoparticles for photocatalytic applications, Appl. Surf. Sci., 448 (2018) 481–488.
[11] E. Mendoza-Mendoza, A.G. Nuñez-Briones, L.A. García-Cerda, R.D. Peralta-Rodríguez, A.J. Montes-Luna, One-step synthesis of ZnO and Ag/ZnO heterostructures and their photocatalytic activity, Ceram. Int., 44 (2018) 6176–6180.
[12] T.P. Chou, Q.F. Zhang, G.E. Fryxell, G.Z. Cao, Hierarchically structured ZnO film for dye sensitized solar cells with enhanced energy conversion efficiency, Adv. Mater., 19 (2007) 2588–2592.
[13] T. Marimuthu, N. Anandhan, Growth and characterization of ZnO nanostructure on $TiO_2$-ZnO films as a light scattering layer for dye sensitized solar cells, Mater. Res. Bull., 95 (2017) 616–624.
[14] L. Pan, T. Muhammad, L. Ma, Z.F. Huang, S.B. Wang, L. Wang, J.J. Zou, X.W. Zhang, MOF-derived C-doped ZnO prepared via a two-step calcination for efficient photo catalysis, Appl. Catal. B: Environ., 189 (2016) 181–191.
[15] N. Kumaresan, K. Ramamurthi, R.R. Babu, K. Sethuraman, S.M. Babu, Hydrothermally grown ZnO nanoparticles for effective photocatalytic activity, Appl. Surf. Sci., 418 (2017) 138–146.
[16] H. Wang, X.Q. Qiu, W.F. Liu, D.J. Yang, Facile preparation of well-combined lignin-based carbon/ZnO hybrid composite with excellent photocatalytic activity, Appl. Surf. Sci., 426 (2017) 206–216.
[17] Y.H. Lu, W.H. Lin, C.Y. Yang, Y.H. Chiu, Y.C. Pu, M.H. Lee, Y.C. Tseng, Y.J. Hsu, A facile green antisolvent approach to $Cu^{2+}$-doped ZnO nanocrystals with visible-light-responsive photo activities, Nanoscale, 6 (2014) 8796–8803.
[18] Y.J. Wang, R. Shi, J. Lin, Y.F. Zhu, Enhancement of photo current and photocatalytic activity of ZnO hybridized with graphite-like $C_3N_4$, Energy. Environ. Sci., 4 (2011) 2922–2929.
[19] K. Bramhaiah, V.N. Singh, N.S. John, Hybrid materials of ZnO nanostructures with reduced graphene oxide and gold nanoparticles: enhanced photo degradation rates in relation to their composition and morphology, Phys. Chem. Chem. Phys., 18 (2016)1478–1486.
[20] C.M. Chou, Y.C. Chang, P.S. Lin, F.K. Liu, Growth of Cu-doped ZnO nanowires or ZnO-CuO nanowires on the same brass foil with high performance photocatalytic activity and stability, Mater. Chem. Phys., 201 (2017) 18–25.
[21] J. Wang, Z. Yang, X.X. Gao, W.Q. Yao, W.Q. Wei, X.J. Chen, R.L. Zong, Y.F. Zhu, Core-shell g-$C_3N_4$@ZnO composites as photo anodes with double synergistic effects for enhanced visible-light photo electro catalytic activities, Appl. Catal. B: Environ., 217 (2017) 169–180.
[22] K.Z. Qi, B. Cheng, J.G. Yu, W.K. Ho, Review on the improvement of the photocatalytic and antibacterial activities of ZnO, J. Alloy. Compd., 727 (2017) 792–820.
[23] G.Q. Li, Z.G. Yi, H.T. Wang, C.H. Jia, W.F. Zhang, Factors impacted on anisotropic photocatalytic oxidization activity of ZnO: Surface band bending, surface free energy and Surface Conductance, Appl. Catal. B: Environ., 158–159 (2014) 280–285.
[24] Y.J. Si, H.H. Liu, N.T. Li, J.B. Zhong, J.Z. Li, D.M. Ma, SDBS-assisted hydrothermal treatment of $TiO_2$ with improved photocatalytic activity, Mater. Lett., 212 (2018) 147–150.
[25] H. Wang, X.Q. Qiu, W.F. Liu, D.J. Yang, Facile preparation of well-combined lignin-based carbon/ZnO hybrid composite with excellent photocatalytic activity, Appl. Surf. Sci., 426 (2017) 206–216.
[26] Q. Yang, J.B. Zhong, J.Z. Li, J.F. Chen, Z. Xiang, T. Wang, M.J. Li, Photo-induced charge separation properties of NiO/$Bi_2O_3$ heterojunctions with efficient simulated solar-driven photocatalytic performance, Curr. Appl. Phys., 17 (2017) 484–487.
[27] J.B. Zhong, J.Z. Li, S.T. Huang, C.Z. Cheng, W. Yuan, M.J. Li, J. Ding, Improved solar-driven photocatalytic performance of $Ag_2CO_3$/$(BiO)_2CO_3$ prepared in-situ, Mater. Res. Bull., 77 (2016) 185–189.
[28] S.T. Huang, J.B. Zhong, J.Z. Li, J.F. Chen, Z. Xiang, W. Hu, M.J. Li, Z-scheme $TiO_2$/g-$C_3N_4$ composites with improved solar-driven photocatalytic performance deriving from remarkably efficient separation of photo-generated charge pairs, Mater. Res. Bull., 84 (2016) 65–70.
[29] X.W. Zheng, Q. Yang, S.T. Huang, J.B. Zhong, J.Z. Li, R.H. Yang, Y.Y. Zhang, Enhanced separation efficiency of photo-induced charge pairs and sunlight-driven photocatalytic performance of $TiO_2$ prepared with the assistance of $NH_4Cl$, J. Sol-Gel Sci. Technol., 83 (2017) 174–180.
[30] J.F. Chen, J.B. Zhong, J.Z. Li, S.T. Huang, M.J. Li, Enhanced photocatalytic activity of C-N-S-tridoped $TiO_2$ towards degradation of methyl orange and phenol, Desal. Water Treat., 75 (2017) 195–201.
[31] J.B. Zhong, J.Z. Li, Y. Lu, X.Y. He, J. Zeng, W. Hu, Y.C. Shen, Fabrication of $Bi^{3+}$-doped ZnO with enhanced photocatalytic performance, Appl. Surf. Sci., 258 (2012) 4929–4933.
[32] J.Z. Li, J.B. Zhong, W. Hu, Y. Lu, J. Zeng, Y.C. Shen, Fabrication of tin-doped zinc oxide by parallel flow co-precipitation with enhanced photocatalytic performance, Mat. Sci. Semicon. Proc., 16 (2013) 143–148.
[33] C.J. Chang, T.L. Yang, Y.C. Weng, Synthesis and characterization of Cr-doped ZnO nanorod-array photo catalysts with improved activity, J. Solid State Chem., 214 (2014) 101–107.
[34] S.H. Hsieh, J.M. Ting, Characterization and photocatalytic performance of ternary Cu-doped ZnO/Graphene materials, Appl. Surf. Sci., 427 (2018) 465–475.

[35] Z. Xiang, J.B. Zhong, S.T. Huang, J.Z. Li, J.F. Chen, T. Wang, M.J. Li, P. Wang, Efficient charge separation of $Ag_2CO_3$/ZnO composites prepared by a facile precipitation approach and its dependence on loading content of $Ag_2CO_3$, Mat. Sci. Semicon. Proc., 52 (2016) 62–67.
[36] L.H. Xu, Y. Zhou, Z.J. Wu, G.G. Zheng, J.J. He, Y.J. Zhou, Improved photocatalytic activity of nanocrystalline ZnO by coupling with CuO, J. Phys. Chem. Solids, 106 (2017) 29–36.
[37] Q. Qi, S.J. Liu, X. Li, C.L. Kong, Z.Y. Guo, L. Chen, In situ fabrication of ZnO@N-doped nanoporous carbon core-shell heterostructures with high photocatalytic and adsorption capacity by a calcination of ZnO@MOF strategy, J. Solid State Chem., 255 (2017) 108–114.
[38] W.W. Yu, T.G. Liu, S.Y. Cao, C. Wang, C.S. Chen, Constructing $MnO_2$/single crystalline ZnO nanorod hybrids with enhanced photocatalytic and antibacterial activity, J. Solid State Chem., 239 (2016) 131–138.
[39] H. Wang, X. Liu, S.L. Wang, L. Li, Dual templating fabrication of hierarchical porous three-dimensional ZnO/carbon nanocomposites for enhanced photocatalytic and photo electrochemical activity, Appl. Catal. B: Environ., 222 (2018) 209–218.
[40] L.H. Yu, W. Chen, D.Z. Li, J.B. Wang, Y. Shao, M. He, P. Wang, X.Z. Zheng Inhibition of photo corrosion and photo activity enhancement for ZnO via specific hollow ZnO core/ZnS shell structure, Appl. Catal. B: Environ., 164 (2015) 453–461.
[41] A.D. Mauro, M.E. Fragalà, V. Privitera, G. Impellizzeri, ZnO for application in photo catalysis: From thin films to nanostructures, Mat. Sci. Semicon. Proc., 69 (2017) 44–51.
[42] N. Kumaresan, K. Ramamurthi, R.R. Babu, K. Sethuraman, S.M. Babu, Hydrothermally grown ZnO nanoparticles for effective photocatalytic activity, Appl. Surf. Sci., 418 (2017) 138–146.
[43] G. Ramakrishna, A. Das, H.N. Ghosh, Effect of surface modification on back electron transfer dynamics of dibromo fluorescein sensitized $TiO_2$ nanoparticles, Langmuir, 20 (2004) 1430–1435.
[44] J.C. Yu, J.G. Yu, J.C. Zhao, Enhanced photocatalytic activity of mesoporous and ordinary $TiO_2$ thin films by sulfuric acid treatment, Appl. Catal. B: Environ., 36 (2002) 31–43.
[45] W. Fei, H. Yang, Y.C. Zhang, Enhanced photocatalytic performance of $CuBi_2O_4$ particles decorated with Ag nanowires, Mat. Sci. Semicon. Proc., 73 (2018) 58–66.
[46] L.J. Di, H. Yang, T. Xian, X.J. Chen, Enhanced photocatalytic activity of $NaBH_4$ reduced $BiFeO_3$ nanoparticles for Rhodamine B decolorization, Mater., 10 (2017) 1118–1128.
[47] L.W. Chen, W.C. Sheng, L.H. Gan, Preparation of $TiO_2$ function film and factors affecting its photocatalytic activity, Funct. Mater., 33 (2002) 246–249.
[48] B. Shirdel, M.A. Behnajady, Sol-gel synthesis of Ba-doped ZnO nanoparticles with enhanced photocatalytic activity in degrading Rhodamine B under UV-A irradiation, Optik, 147 (2017) 143–150.
[49] J.B. Zhong, J.Z. Li, F.M. Feng, Y. Lu, J. Zeng, W. Hu, Z. Tang, Improved photocatalytic performance of $SiO_2$-$TiO_2$ prepared with the assistance of SDBS, J. Mol. Catal. A: Chem., 357 (2012) 101–105.
[50] L.Q. Ye, J.Y. Liu, Z. Jiang, T.Y. Peng, L. Zan, Facets coupling of BiOBr-g-$C_3N_4$ composite photo catalyst for enhanced visible-light-driven photocatalytic activity, Appl. Cataly. B: Environ., 142–143 (2013) 1–7.
[51] X.L. Liu, J.B. Zhong, J.Z. Li, S.T. Huang, W. Song, PEG-assisted hydrothermal synthesis of BiOCl with enhanced photocatalytic performance, Appl. Phys., A 119 (2015) 1203–1208.
[52] M. Yang, Q. Yang, J.B. Zhong, J.Z. Li, S.T. Huang, X.J. Li, PVA-assisted hydrothermal preparation of BiOF with remarkably enhanced photocatalytic performance, Mater. Lett., 201 (2017) 35–38.
[53] S.T. Huang, J.F. Chen, J.B. Zhong, J.Z. Li, W. Hu, M.J. Li, Enhanced photocatalytic performance of Ag/AgCl/$SnO_2$ originating from efficient formation of $^{\bullet}O_2^-$, Mater. Chem. Phys. 201 (2017) 35–41.
[54] X.W. Zheng, H.H. Liu, J.B. Zhong, S.T. Huang, J.Z. Li, D.M. Ma, Remarkably enhanced sunlight-driven photocatalytic performance of $TiO_2$ by facilely modulating the surface property, Mat. Sci. Semicon. Proc., 74 (2018) 109–115.
[55] J.B. Zhong, J.Z. Li, Z.H. Xiao, W. Hu, X.B. Zhou, X.W. Zheng, Improved photocatalytic performance of ZnO prepared by sol-gel method with the assistance of CTAB, Mater. Lett., 91 (2013) 301–303.
[56] L. Kronik, Y. Shapira, Surface photo voltage phenomena: theory, experiment and application, Surf. Sci. Rep., 254 (1999) 1–205.
[57] X. Zhao, H. Yang, Z. Cui, R. Li, W. Feng, Enhanced photocatalytic performance of Ag-$Bi_4Ti_3O_{12}$ nanocomposites prepared by a photocatalytic reduction method, Mater. Technol., 32 (2017) 870–880.
[58] L.Q. Ye, K.J. Deng, F. Xu, L.H. Tian, T.Y. Peng, L. Zan, Increasing visible-light absorption for photo catalysis with black BiOCl, Phys. Chem. Chem. Phys., 14 (2011) 82–85.
[59] W.Z. Wang, G.H. Wang, X.S. Wang, Y.J. Zhan, Y.K. Liu, C.L. Zheng, Synthesis and characterization of $Cu_2O$ nanowires by a novel reduction route, Adv. Mater., 14 (2002) 67–69.
[60] W. Sun, W.D. Sun, Y.J. Zhuo, Y. Chu, Facile synthesis of $Cu_2O$ nanocube/polycarbazole composites and their high visible-light photocatalytic properties, J. Solid State Chem., 184 (2011) 1638–1643.
[61] X.D. Su, J.Z. Zhao, Y.L. Li, Y.C. Zhu, X.K. Ma, F. Sun, Z.C. Wang, Solution synthesis of $Cu_2O$/$TiO_2$ core-shell nanocomposites, Colloids Surf., A 349 (2009) 151–155.
[62] G. Li, D. Zhang, J.C. Yu, Thermally stable ordered mesoporous $CeO_2$/$TiO_2$ visible-light photo catalysts, Phys. Chem. Chem. Phys., 11 (2009) 3775–3782.
[63] J.X. Shu, Z.H. Wang, Y.J. Huang, N. Huang, C.G. Ren, W. Zhang, Adsorption removal of Congo red from aqueous solution by polyhedral $Cu_2O$ nanoparticles: kinetics, isotherms, thermodynamics and mechanism analysis, J. Alloy. Compd. 633 (2015) 338–346.
[64] J.D. Ye, S.L. Gu, F. Qin, S.M. Zhu, S.M. Liu, X. Zhou, W. Liu, L.Q. Hu, R. Zhang, Y. Shi, Y.D. Zheng, Y.D. Ye, MOCVD growth and properties of ZnO films using dimethylzinc and oxygen, Appl. Phys. A. Mater., 81 (2005) 809–812.
[65] K. Ebitani, H. Konno, T. Tanaka, H. Hattori, In-situ XPS study of zirconium oxide promoted by platinum and sulfate ion, J. Catal., 135 (1992) 60–67.
[66] M.R. Hoffmann, S.T. Martin, W. Choi, D.W. Bahnemann, Environmental applications of semiconductor photo catalysis, Chem. Rev., 95 (1995) 69–96.
[67] J.F. Chen, J.B. Zhong, J.Z. Li, J. Zeng, S.T. Huang, L. Dou, Photo induced charge separation and simulated solar-driven photocatalytic performance of C-N-co-doped $TiO_2$ prepared by sol-gel method, J. Sol-Gel Sci. Technol., 76 (2015) 332–340.